Published in final edited form as:
Dent Mater. 2014 July ; 30(7): e199–e207. doi:10.1016/j.dental.2014.03.008.

Bone regeneration via novel macroporous CPC scaffolds in critical-sized cranial defects in rats

Kangwon Lee[1,*], **Michael D. Weir**[2,*], **Evi Lippens**[1,*], **Manav Mehta**[1], **Ping Wang**[2], **Georg N. Duda**[3], **Woo S. Kim**[1], **David J. Mooney**[1], and **Hockin H. K. Xu**[2,4,5,6]

[1]School of Engineering and Applied Sciences, Harvard University, Cambridge, MA 02138, USA

[2]Biomaterials & Tissue Engineering Division, Department of Endodontics, Prosthodontics and Operative Dentistry, University of Maryland School of Dentistry, Baltimore, MD 21201, USA

[3]Julius Wolff Institute, Charité - Universitätsmedizin Berlin and Berlin-Brandenburg Center for Regenerative Therapies, Berlin, Germany

[4]Center for Stem Cell Biology and Regenerative Medicine, University of Maryland School of Medicine, Baltimore, MD 21201, USA

[5]Marlene and Stewart Greenebaum Cancer Center, University of Maryland School of Medicine, Baltimore, MD 21201, USA

[6]Department of Mechanical Engineering, University of Maryland, Baltimore County, MD 21250, USA

Abstract

Objectives—Calcium phosphate cement (CPC) is promising for dental and craniofacial applications due to its ability to be injected or filled into complex-shaped bone defects and molded for esthetics, and its resorbability and replacement by new bone. The objective of this study was to investigate bone regeneration via novel macroporous CPC containing absorbable fibers, hydrogel microbeads and growth factors in critical-sized cranial defects in rats.

Methods—Mannitol porogen and alginate hydrogel microbeads were incorporated into CPC. Absorbable fibers were used to provide mechanical reinforcement to CPC scaffolds. Six CPC groups were tested in rats: (1) Control CPC without macropores and microbeads; (2) Macroporous CPC + large fiber; (3) Macroporous CPC + large fiber + nanofiber; (4) Same as (3), but with rhBMP2 in CPC matrix; (5) Same as (3), but with rhBMP2 in CPC matrix + rhTGF-β1 in microbeads; (6) Same as (3), but with rhBMP2 in CPC matrix + VEGF in microbeads. Rats were sacrificed at 4 and 24 weeks for histological and micro-CT analyses.

Correspondence: Dr. Hockin H. K. Xu, Professor, Director of Biomaterials & Tissue Engineering Division, Department of Endodontics, Prosthodontics and Operative Dentistry, University of Maryland School of Dentistry, Baltimore, MD 21201 (hxu@umaryland.edu).
*These authors contributed equally to this study.

Results—The macroporous CPC scaffolds containing porogen, absorbable fibers and hydrogel microbeads had mechanical properties similar to cancellous bone. At 4 weeks, the new bone area fraction (mean ± sd; n = 5) in CPC control group was the lowest at (14.8 ± 3.3)%, and that of group 6 (rhBMP2 + VEGF) was (31.0 ± 13.8)% ($p < 0.05$). At 24 weeks, group 4 (rhBMP2) had the most new bone of (38.8 ± 15.6)%, higher than (12.7 ± 5.3)% of CPC control ($p < 0.05$). Micro-CT revealed nearly complete bridging of the critical-sized defects with new bone for several macroporous CPC groups, compared to much less new bone formation for CPC control.

Significance—Macroporous CPC scaffolds containing porogen, fibers and microbeads with growth factors were investigated in rat cranial defects for the first time. Macroporous CPCs had new bone up to 2-fold that of traditional CPC control at 4 weeks, and 3-fold that of traditional CPC at 24 weeks, and hence may be useful for dental, craniofacial and orthopedic applications.

Keywords

Calcium phosphate cement; macroporous scaffold; strength and toughness; bone regeneration; growth factors; critical-sized cranial defects

1. Introduction

Bone defects are a worldwide problem, and the need for bone repair arises due to trauma, tumor ablative surgery, congenital defects, infectious conditions and other causes of loss of skeletal tissue [1-7]. Furthermore, the need for bone repair is increasing rapidly due to an aging population with increased life expectancies and diseases such as osteoporosis [3,8,9]. In particular, the supply of bone grafts to treat critical-sized bone defects remains a major challenging health issue worldwide [10]. Although autograft and allograft transplantations are used clinically, their disadvantages include donor site morbidity, harvesting limitation, and disease transmission risks. Biomaterials are a promising alternative for bone repair. While bioinert implants can induce fibrous-capsules, bioactive implants with bone-like calcium phosphate (CaP) minerals can bond to bone to form a functional interface. CaP minerals enhance cell attachment and osteoblastic phenotype expression, and hence are important for bone repair [11-17].

For sintered bioceramics to fit into a bone cavity, the surgeon needs to machine the graft or carve the surgical site, leading to increases in bone loss, trauma, and surgical time. Calcium phosphate cements can be molded to achieve esthetics in craniofacial repairs, and set *in situ* to provide intimate adaptation to complex-shaped defects [9,13,18-20]. One such cement is comprised of tetracalcium phosphate (TTCP) and dicalcium phosphate-anhydrous (DCPA) and is referred to as CPC [18,21]. The CPC powder can be mixed with an aqueous liquid to form a paste that can be sculpted during surgery to conform to the defects in hard tissues. The paste self-hardens to form resorbable hydroxyapatite [18,21]. Traditional CPC was mechanically weak, hence absorbable fibers and chitosan were used to reinforce the CPC scaffold [22,23]. Chitosan enabled CPC to be fast-setting and washout-resistant [23]. Macropores were created in CPC using water-soluble mannitol porogen to enhance cell infiltration [23]. Recently, alginate microbeads were incorporated into CPC as a potential vehicle for growth factor/cell delivery, and the CPC paste containing microbeads and reinforcement fibers was fully injectable [24]. Macroporous CPC scaffold is promising for a

variety of dental and craniofacial applications, including mandibular and maxillary ridge augmentation and periodontal bone repair, since CPC could be molded to the desired shape and set to form a scaffold for bone ingrowth. Other applications include the major reconstructions of the maxilla or mandible after trauma or tumor resection, as well as the support of metal dental implants or augmentation of deficient implant sites, and the repair of cranial defects. However, previous studies on macroporous CPC focused on in vitro experiments [22-24], without testing in animal models.

The objective of this study was to investigate bone regeneration via macroporous CPC containing absorbable fibers, microbeads and growth factors in a critical-sized cranial defect model in rats. It was hypothesized that: (1) While macropores will weaken the CPC mechanically, fiber reinforcement will increase the strength of CPC; (2) New bone formation will be increased via the macropores in CPC, and the new bone area fraction in the cranial defect will be increased via the incorporation of recombinant human bone morphogenetic protein-2 (rhBMP2), vascular endothelial growth factor (VEGF) and recombinant human transforming growth factor-β1 (rhTGF-β1) incorporated into CPC scaffolds.

2. Materials and methods

2.1. CPC composite scaffold fabrication

TTCP ($Ca_4(PO_4)_2O$) was synthesized from a solid-state reaction at 1500 °C between DCPA ($CaHPO_4$) and $CaCO_3$ (J. T. Baker, Phillipsburg, NJ). The mixture was ground to obtain TTCP particles with sizes of 1-80 μm, with a median particle size of 17 μm. DCPA was ground to obtain particles with sizes of 0.4-3.0 μm, with a median particle size of 1.0 μm. The TTCP and DCPA were then mixed to form the CPC powder. Traditionally, the TTCP/DCPA molar ratio was 1/1 [18,21]. Recently, a TTCP/DCPA ratio of 1/3 was shown to yield CPC with strength similar to that using 1/1, while the 1/3 ratio had faster dissolution which indicates potentially faster resorption *in vivo* [25]. Hence, in this study, the CPC control used a TTCP/DCPA ratio of 1/1, while the other groups used a TTCP/DCPA ratio of 1/3. Hence the TTCP/DCPA ratio of the CPC control was the same as the CPC in previous *in vivo* studies [21]. Previous studies incorporated water-soluble mannitol into CPC to create macropores [23], and alginate microbeads into CPC as drug and cell carriers [24]. While macroporous CPC was mechanically-weaker than CPC without macropores, chitosan and fibers were incorporated into CPC for reinforcement. Therefore, for mechanical testing, four CPCs were made: (i) CPC control (without mannitol or microbeads); (ii) macroporous CPC with 30% mannitol, 30% alginate microbeads, and 15% chitosan in CPC liquid (referred to as “macroporous CPC”); (iii) Same as (ii), but with 15% large-diameter absorbable fibers (“macroporous CPC + large fiber”); (iv) Same as (ii), but with 7.5% large-diameter fibers + 7.5% nanofibers (“macroporous CPC + large fiber + nanofiber”).

Alginate hydrogel microbeads were synthesized using a previously-described method [26]. First, the alginate was oxidized to increase its degradability in vivo [27]. Oxidation was performed using sodium periodate at the correct stoichiometric ratio of sodium periodate/alginate to have certain percentages of alginate oxidation [27]. The percentage of oxidation (%) was the number of oxidized uronate residues per 100 uronate units in the alginate chain.

Alginate at 7.5% oxidation was synthesized as described previously [26]. Briefly, 1% of sodium alginate was dissolved in water. Then 1.51 mL of 0.25 mol/L sodium periodate (Sigma-Aldrich) was added to 100 mL alginate solution. At 24 h, the oxidization reaction was stopped by adding 1 g of ethylene glycol and then 2.5 g of sodium chloride. The precipitates were re-dissolved and the second precipitates were collected. The oxidized alginate thus obtained was dissolved in saline at a concentration of 1.2%. The solution was loaded into a bead-generating device (Var-J1, Nisco, Zurich, Switzerland). The droplets fell into a well of 100 mmol/L calcium chloride and crosslinked to form microbeads. The microbeads were slightly elongated with a mean length of 335 μm and a mean diameter of 232 μm as measured previously [26].

A suture fiber (Vicryl, Ethicon, Somerville, NJ) was cut to 3 mm filaments. This suture consisted of fibers braided into a bundle with a diameter of 322 μm, suitable for producing long cylindrical macropores after fiber dissolution in CPC. Chitosan malate (Vanson, Redmond, WA) was mixed with water at a chitosan/(chitosan + water) mass fraction of 15% to form the CPC liquid. Nanofibers of poly(D,L-lactide-*co*-glycolide) (PLGA) at a poly(lactic acid) (PLA)/poly(glycolic acid) (PGA) ratio of 50/50 were electrospun into non-woven mats, following a previous study [28]. The mat was cut into 3 × 3 mm squares, because a previous study showed that 3 mm fibers in CPC were injectable through a 10-gauge needle [24]. Another study also cut electrospun fibers into 3 mm dimensions for use in CPC [29]. CPC powder and liquid were mixed at a mass ratio of 2:1, and the prescribed amounts of fibers and microbeads were mixed with the CPC-chitosan paste. The mixed composite paste was placed into 3 × 4 × 25 mm molds and set at 100% humidity for 4 h at 37 °C. The specimens were then demolded and immersed in water at 37 °C for 20 h.

2.2. Mechanical testing

A three-point flexural test was performed using a 20 mm span and a displacement rate of 1 mm/min to measure the mechanical properties of CPC. Flexural strength was calculated as $S = 3F_{max}L/(2bh^2)$, where F_{max} is the maximum load, L is the span, b is specimen width, and h is specimen thickness. Elastic modulus was calculated as $E = (F/c)(L^3/[4bh^3])$, where load F divided by displacement c is the slope of the load-displacement curve in the linear elastic region. Work-of-fracture (toughness) was measured as the area of the load-displacement curve divided by the specimen's cross-sectional area [23].

2.3. Critical-sized cranial defect model in rats

The mechanical property results showed that the macroporous CPC group (ii) was much weaker than CPC control (i). However, fiber reinforcement rendered the macroporous CPC (iii and iv) to have similar strengths to CPC control. Therefore, for the animal study, the following six groups were tested:

1. Control CPC without macropores and microbeads (similar to the CPC in previous *in vivo* studies, such as Friedman *et al.*, 1998);
2. Macroporous CPC + large fiber (30% mannitol, 30% alginate microbeads, 15% chitosan in cement liquid, reinforced with 15% large-diameter Vicryl fibers);

3. Macroporous CPC + large fiber + nanofiber (same as 2, except reinforcement with 7.5% Vicryl fibers + 7.5% nanofibers);
4. Same as (3), but with rhBMP2 in the CPC matrix;
5. Same as (3), but with rhBMP2 in the CPC matrix + rhTGF-β1 in the microbeads;
6. Same as (3), but with rhBMP2 in the CPC matrix + VEGF in the microbeads.

rhBMP2, VEGF and rhTGF-β1 were commercially-obtained (PeproTech, Rocky Hill, NJ). Their amounts were 10 μg rhBMP2/defect, 6 μg VEGF/defect, and 200 ng rhTGF-β1/defect, selected following previous studies [30-32].

The rat critical-sized cranial defect model was approved by Harvard University (# 24-09) and University of Maryland (# 0909014). NIH procedures were followed. Surgery was performed at Harvard University. Lewis rats (age: 49-55 days, Charles River, Wilmington, MA) were anesthetized by intraperitoneal injection (40-90 mg/kg ketamine; 5-15 mg/kg xylazine). A mid-longitudinal incision was made on the dorsal surface of cranium (the periosteum was removed). A trephine bur was used to create a circular defect with a diameter of 8 mm at full thickness of 1 to 1.5 mm. A CPC paste (0.2 g) was placed between two glass plates to yield a thickness of approximately 1 mm. The paste was shaped as a disk with a diameter of 8 mm and placed into the defect. After 4 or 24 weeks, the animals were sacrificed with carbon monoxide [15,33]. Six groups of scaffolds, with n = 5, required 60 rats.

2.4. Histological and micro-CT analyses

For each rat, the implant with surrounding native bone was retrieved. The tissues were fixed for 24 h at 4 °C in 10% phosphate-buffered formalin. Following fixation, implants were analyzed by micro CT (μCT) following previous studies [15,33]. The rat skull was wrapped in a moistened cotton mesh and placed in a custom-built radiolucent batch scanning acrylic tube. The scans were performed on a Viva40 μCT (Scanco Medical AG), at a voltage of 55 kV, current of 145 μA, and integration time of 314 ms. Voxel size was selected to be isotropic and fixed at 35.5 μm. The scan axis was normal to the subject frontal plane [15,33]. Subsequently, the whole skull was decalcified in a weak (15%) buffered formic acid and trimmed to a section of 1 mm in front of the defect and 1 mm behind the defect. This strip of skull bone with the defect in the middle was processed and embedded in paraffin. Using a microtome, 5 mm of the samples was cut away to transfer 5 μm thick sections from the central area of the original defect site onto a glass slide. These sections were stained with hematoxylin and eosin (H&E) (Mass Histology Service, Worcester, MA). The new bone and original implantation areas were calculated by Image J (NIH) software. The new bone area fraction was measured as the new bone area/original total implant area.

2.5. Statistical analysis

One-way and two-way nonparametric Mann-Whitney tests were performed to detect significant effects of the variables. Tukey's multiple comparison tests were used at $p = 0.05$.

3. Results

The mechanical properties of CPC scaffolds are plotted in Fig. 1. In each plot, values with dissimilar letters are significantly different from each other ($p < 0.05$). The creation of macropores in CPC decreased the flexural strength compared to CPC control ($p < 0.05$). However, adding fibers to CPC increased the strength back to a level similar to that of CPC control without macropores ($p > 0.1$). Therefore, macropores could be created in CPC without compromising the strength, compared to CPC control. There was no significant difference between the two groups with large-diameter fibers or a combination of large-diameter fibers and nanofibers ($p > 0.1$). Elastic modulus was also increased via fiber reinforcement, compared to that of macroporous CPC without fibers. Due to fiber reinforcement, the work-of-fracture of macroporous CPC was higher than CPC control without fibers ($p < 0.05$).

All CPC samples showed resorption in vivo with new bone formation at 4 and 24 weeks. There was more new bone formation in the macroporous CPC groups than CPC control. Typical examples are shown in Fig. 2A-C at 24 weeks for groups 3, 5 and 6, respectively. The six groups had similar histological features with variations in the amounts of new bone. New bone originated both endogenously from the defect margins, and in some samples from the foci of new bone in the defect center. Fig. 2D shows new bone formation around the CPC residues in group 1. In addition to new bone and CPC residues, new blood vessels (BV) also formed in the defects, with an example shown for group 2 in Fig. 2E. Other groups had similar formation of blood vessels. In addition, alginate hydrogel residues ("H" in Fig. 2E) were present in defects, indicating that the alginate microbeads had not fully resorbed at 24 weeks in vivo. Alginate residues were observed in other groups too; in Fig. 2F, the alginate residues were stained red for group 4.

The new bone area fraction was measured as the new bone area divided by the total area of the defect in Fig. 3: (A) 4 weeks, and (B) 24 weeks. At 4 weeks, the new bone area fraction in group 1 was the lowest $(14.8 \pm 3.3)\%$. The macroporous CPC groups had new bone area fractions of 24-34%. Groups 3 and 6 had significantly more new bone than group 1 ($p < 0.05$). The new bone area fraction in group 6 was $(31.0 \pm 13.8)\%$, which was 2-fold that of CPC control in group 1.

At 24 weeks (Fig. 3B), the new bone area fraction for groups 2 and 3 progressively increased over that of group 1. Group 4 had the most new bone area fraction of $(38.8 \pm 15.6)\%$, which was 3-fold the $(12.7 \pm 5.3)\%$ of CPC control in group 1 ($p < 0.05$). Statistically, groups 3-5 had significantly more new bone area fraction than group 1 ($p < 0.05$).

Representative images from μCT of the cranial defects in rats are shown in Fig. 4 at 24 weeks. Based on the morphology of structures in the defects, it is possible to infer that the isolated islands of particulates in the defects were a combination of CPC and newly-formed bone. The white arrow in (A) indicates examples of the CPC residues inside the defect. The black arrow in (B) indicates examples of new bony islands in the defect which had a more cohesive structure with new bone morphology. Examination of all samples indicated that

more new bone had formed in samples with macroprous CPC and the incorporation of growth factors, compared to CPC control. For example, in (C) and (D) for groups 3 and 4, the defects were almost completely bridged with new bone. These observations are consistent with and support the quantitative results in Fig. 3.

4. Discussion

Macroporous CPC scaffolds containing mannitol, alginate microbeads and absorbable fibers were investigated for *in vivo* bone regeneration for the first time. The mannitol porogen particles could dissolve after 1-day immersion to create macropores in CPC, as shown previously [23]. The alginate hydrogel microbeads had the potential to deliver growth factors and stem cells as shown in a previous study [24], although such an investigation in vivo would require a separate study. CPC is injectable, can be molded to a desirable shape and set to form a moderately load-bearing scaffold [24]. Previous studies reported that the strength was 0.7 MPa for currently-available injectable polymeric carriers for delivering growth factors and cells [34], and 0.1 MPa for hydrogels [35,36]. Elastic modulus was 8 MPa for injectable polymeric carrier and 0.1 MPa for hydrogels. It was concluded that "Hydrogel scaffolds…do not possess the mechanical strength to be used in load bearing applications" [37]. In the present study, the macroporous CPC scaffold had a strength of about 4 MPa, matching the reported 3.5 MPa for cancellous bone [38]. Macroporous CPC had elastic modulus of about 500 to 1000 MPa, which compares with the reported elastic modulus of approximately 300 MPa for cancellous bone [39]. A literature search did not found the work-of-fracture value of cancellous bone. For cortical bone, the work-of-fracture was measured to have a range of approximately 300 to 2300 J/m^2 [40]. Hence, the fiber-reinforced macroporous CPC's work-of-fracture of approximately 500 J/m^2 (Fig. 1C) approached the lower end of that for cortical bone. The mechanical property increase for macroporous CPC was likely due to the fibers bridging the cracks and rendering further crack opening and propagation more difficult, thus improving the fracture resistance of the scaffold [22,23]. Therefore, the CPC scaffolds containing mannitol, microbeads and fibers possessed strength and modulus that were much higher than the previous injectable carriers, and approached those of cancellous bone.

After 4 weeks in vivo, the CPC control yielded 14.8% of new bone area fraction in the critical-sized cranial defects in rats, while group 6 generated a much higher new bone area fraction of 31%. After 24 weeks in vivo, CPC control had a new bone area fraction of 12.7%, while group 4 generated 38.8% new bone. There was no increase of new bone for CPC control from 4 to 24 weeks. A similar trend was observed in a previous study in sheep, where CPC generated 28.3% of new bone at 12 weeks; however, it then plateaued, with 27.8% of new bone at 24 weeks [41]. In general, the new bone amounts of the present study are consistent with those in previous reports. For example, using 8-mm cranial defects in rats, a previous study showed that CPC containing BMP-2 generated (9 ± 4)% of new bone at 2 weeks, versus (8 ± 4)% without BMP-2 [32]. The new bone area fractions were higher at 10 weeks: (53 ± 5)% for CPC with BMP-2, compared to (43 ± 10%) for CPC without BMP-2 [32]. Another previous study reported new bone percentages of (5.5 ± 0.4)% and (8.1 ± 1.3)% at 4 weeks using CPC control and BMP-2-loaded CPC, respectively [42]. The new bone percentages then increased at 12 weeks to (10 ± 3)% and (16 ± 2)% for CPC

control and BMP-2-loaded CPC, respectively [42]. Previous studies on the use of CPC in animal models indicated that the new bone amounts varied in different studies. For example, one previous study reported new bone formation via CPC of (12.4 ± 2.7)% at 12 months [43]. Another study reported (34 ± 4)% of new bone fraction at 3 months [44]. These differences are likely caused by differences in species and ages of the animals, anatomical site, implantation method and time duration, chemical composition and microstructure of the CPC scaffold, and the incorporation of various growth factors.

Groups 3 and 6 formed significantly more new bone than CPC control at 4 weeks. Group 3 contained macropores, and group 6 had rhBMP2 in the CPC matrix and VEGF in the alginate hydrogel microbeads. The macropores could facilitate cell infiltration and tissue ingrowth, and enhance scaffold resorption. The presence of macropores and growth factors in CPC likely contributed to the greater new bone amount at 4 weeks. At 24 weeks, groups 3-5 formed much more bone than CPC control. Group 4 had rhBMP2 in the CPC matrix, and group 5 contained rhBMP2 in the CPC matrix and rhTGF-β1 in the microbeads. These factors appeared to have promoted bone regeneration compared to CPC control. The new bone amount was increased by 2-fold at 4 weeks, and 3-fold at 24 weeks, when comparing between the best macroporous CPC groups and the CPC control.

Bone development and regeneration in vivo are regulated by a series of growth factors [45]. BMP2 is one of the most widely studied growth factors in bone regeneration with confirmed and strong osteoinductive potential [42,46,47], and has been approved by the Food and Drug Administration's Medical Device Panel for clinical use [48]. TGF-β1 has been reported as a multipotent regulator of cell metabolism and differentiation in a number of cell types, and can enhance bone formation and contribute to neovascularization [30,49,50]. VEGF has been shown to enhance angiogenesis and bone formation [15,51,52], and can function not only as a potent factor to modulate endothelial cells and promote angiogenesis [53], but also as a stimulant for osteoblast chemotaxis and differentiation [54]. These are the reasons that rhBMP-2, rhTGF-β1 and VEGF were selected in the present study. Furthermore, it is desirable to deliver more than one growth factor. Indeed, a recent study showed that when BMP2 and TGF-β1 were delivered together, there was significantly more bone formation than when they were delivered separately [31]. When two or more factors are incorporated into a carrier, they are released simultaneously. However, it is desirable to mimic the nature's delivery of multiple growth factors in a programmed, sequential way. For example, angiogenic agents may be initially needed for a relatively short time until the induction of a vasculature, while the sustained release of BMPs may be required for more durable activity [55]. Therefore, in the present study, rhBMP2 was mixed into the CPC matrix with the purpose of a sustained effect, while TGF-β1 and VEGF were incorporated into the hydrogel mcrobeads. Because the alginate concentration was 1.2%, the microbeads consisted of 98.8% saline, to potentially have a relatively faster release of TGF-β1 and VEGF. However, the addition of growth factors did not increase the new bone formation in the present study. Several reasons may have contributed to this result. First, CPC had a high binding affinity for proteins, exhibiting a high retention of growth factors [56]. While the released growth factors could stimulate and recruit neighboring cells, the bound growth factors could only work over a small distance. Second, the bound growth factors inside CPC may become inactivated over time. For example, a previous study investigating the bioactivity of growth

factors showed that the growth factor released after 24 h did not increase the osteogenesis, but the growth factor released after 1 h did increase the osteogenesis [57]. Therefore, due to the high retention of growth factors in CPC, the portion of released growth factors may have a concentration that was too low for cells to sense, and the growth factors released after an initial time period may have lost the bioactivity. Third, alginate hydrogel residues were observed in the defects. Oxidized alginate microbeads still had a slow degradation, while a recent study showed that adding fibrin to the oxidized alginate microbeads achieved a much faster degradation [26]. Therefore, further study should incorporate the fast-degradable alginate-fibrin microbeads into CPC to release growth factors and create macropores at a faster rate in vivo. Fourth, the incorporation of chitosan in CPC might slow the CPC resorption and new bone formation in vivo, as indicated in a previous study [58]. Further study should use fiber-reinforced macroporous CPC without chitosan to investigate whether the new bone formation rate could be further increased.

5. Conclusions

Macroporous CPC scaffolds containing porogen, fibers and hydrogel microbeads with growth factors were investigated in rat cranial defects for the first time. These novel macroporous scaffolds had mechanical properties similar to cancellous bone, and similar to CPC control without macropores. Macroporous CPC groups had new bone amounts up to 2-fold that of traditional CPC control at 4 weeks, and 3-fold of CPC control at 24 weeks. Macropores and rhBMP2 in CPC progressively increased the amount of new bone formation. However, further adding VEGF and rhTGF-β1 did not further increase the new bone formation, possibly due to growth factor binding to the CPC matrix and growth factor inactivation over time, which require further study. Macroporous CPC with growth factors generated 2-3 fold of new bone than traditional CPC and hence may be useful to promote bone regeneration in dental, craniofacial and orthopedic applications.

Acknowledgments

We thank Drs. Laurence C. Chow and Wenchuan Chen for useful discussions. This study was supported by NIH grant R01 DE14190 (HX) and University of Maryland Dental School.

References

1. Lavik E, Langer R. Tissue engineering: Current state and perspectives. Applied Microbiol & Biotech. 2004; 65:1–8.
2. Bohner M, Gbureck U, Barralet JE. Technological issues for the development of more efficient calcium phosphate bone cements: a critical assessment. Biomaterials. 2005; 26:6423–6429. [PubMed: 15964620]
3. Mikos AG, Herring SW, Ochareon P, Elisseeff J, Lu HH, Kandel R, Schoen FJ, Toner M, Mooney D, Atala A, van Dyke ME, Kaplan D, Vunjak-Novakovic G. Engineering complex tissues. Tissue Eng. 2006; 12:3307–3339. [PubMed: 17518671]
4. Mao JJ, Giannobile WV, Helms JA, Hollister SJ, Krebsbach PH, Longaker MT, Shi S. Craniofacial tissue engineering by stem cells. J Dent Res. 2006; 85:966–979. [PubMed: 17062735]
5. Johnson PC, Mikos AG, Fisher JP, Jansen JA. Strategic directions in tissue engineering. Tissue Eng. 2007; 13:2827–2837. [PubMed: 18052823]
6. The Burden of Musculoskeletal Diseases in the United States. Rosemont, IL: American Academy of Orthopaedic Surgeons; 2008. United States Bone and Joint Decade (USBJD) 2002-2011. Foreword

7. Nie H, Lee CH, Tan J, Lu C, Mendelson A, Chen M, Embree MC, Kong K, Shah B, Wang S, Cho S, Mao JJ. Musculoskeletal tissue engineering by endogenous stem cells. Cell & Tissue Research. 2012; 347:665–676. [PubMed: 22382390]
8. Mao JJ, Stosich MS, Moioli E, Lee CH, Fu SY, Bastian B, Eisig SB, Zemnick C, Ascherman J, Wu J, Rohde C, Ascherman J. Facial reconstruction by biosurgery: cell transplantation vs. cell homing. Tissue Engineering Part B. 2010; 16:257–262.
9. Bohner M. Design of ceramic-based cements and putties for bone graft substitution. Eur Cell Mater. 2010; 20:1–12. [PubMed: 20574942]
10. Meinel L, Karageorgiou V, Fajardo R, Snyder B, Shinde-Patil V, Zichner L, Kaplan D, Langer R, Vunjak-Novakovic G. Bone tissue engineering using human mesenchymal stem cells: effects of scaffold material and medium flow. Ann Biomed Eng. 2004; 32:112–122. [PubMed: 14964727]
11. Pilliar RM, Filiaggi MJ, Wells JD, Grynpas MD, Kandel RA. Porous calcium polyphosphate scaffolds for bone substitute applications -- in vitro characterization. Biomaterials. 2001; 22:963–972. [PubMed: 11311015]
12. Foppiano S, Marshall SJ, Marshall GW, Saiz E, Tomsia AP. The influence of novel bioactive glasses on in vitro osteoblast behavior. J Biomed Mater Res A. 2004; 71:242–249. [PubMed: 15372470]
13. Ginebra MP, Traykova T, Planell JA. Calcium phosphate cements as bone drug-delivery systems: a review. J Controlled Release. 2006; 113:102–110.
14. Deville S, Saiz E, Nalla RK, Tomsia AP. Freezing as a path to build complex composites. Science. 2006; 311:515–518. [PubMed: 16439659]
15. Leach JK, Kaigler D, Wang Z, Krebsbach PH, Mooney DJ. Coating of VEGF-releasing scaffolds with bioactive glass for angiogenesis and bone regeneration. Biomaterials. 2006; 27:3249–3255. [PubMed: 16490250]
16. Reilly GC, Radin S, Chen AT, Ducheyne P. Differential alkaline phosphatase responses of rat and human bone marrow derived mesenchymal stem cells to 45S5 bioactive glass. Biomaterials. 2007; 28:4091–4097. [PubMed: 17586040]
17. Link DP, van den Dolder J, van den Beucken JJ, Wolke JG, Mikos AG, Jansen JA. Bone response and mechanical strength of rabbit femoral defects filled with injectable CaP cements containing TGF-1 loaded gelatin microparticles. Biomaterials. 2008; 29:675–682. [PubMed: 17996293]
18. Brown, WE.; Chow, LC. A new calcium phosphate water setting cement. In: Brown, PW., editor. Cements research progress. Westerville, OH: American Ceramic Society; 1986. p. 352-379.
19. Barralet JE, Gaunt T, Wright AJ, Gibson IR, Knowles JC. Effect of porosity reduction by compaction on compressive strength and microstructure of calcium phosphate cement. J Biomed Mater Res B. 2002; 63:1–9.
20. Bohner M, Baroud G. Injectability of calcium phosphate pastes. Biomaterials. 2005; 26:1553–1563. [PubMed: 15522757]
21. Friedman CD, Costantino PD, Takagi S, Chow LC. BoneSource hydroxyapatite cement: a novel biomaterial for craniofacial skeletal tissue engineering and reconstruction. J Biomed Mater Res B. 1998; 43:428–432.
22. Xu HHK, Quinn JB, Takagi S, Chow LC, Eichmiller FC. Strong and macroporous calcium phosphate cement: Effects of porosity and fiber reinforcement. J Biomed Mater Res. 2001; 57:457–466. [PubMed: 11523041]
23. Xu HHK, Takagi S, Quinn JB, Chow LC. Fast-setting and anti-washout calciumphosphate scaffolds with high strength and controlled macropore formation rates. J BiomedMater Res A. 2004; 68:725–734.
24. Zhao L, Weir MD, Xu HHK. An injectable calcium phosphate - alginate hydrogel - umbilical cord mesenchymal stem cell paste for bone tissue engineering. Biomaterials. 2010; 31:6502–6510. [PubMed: 20570346]
25. Xu HHK, Zhao L, Detamore MS, Takagi S, Chow LC. Umbilical cord stem cell seeding on fast-resorbable calcium phosphate bone cement. Tissue Engineering A. 2010; 16:2743–2753.
26. Zhou H, Xu HHK. The fast release of stem cells from alginate-fibrin microbeads in injectable scaffolds for bone tissue engineering. Biomaterials. 2011; 32:7503–7513. [PubMed: 21757229]

27. Bouhadir KH, Lee KY, Alsberg E, Damm KL, Anderson KW, Mooney DJ. Degradation of partially oxidized alginate and its potential application for tissue engineering. Biotech Progress. 2001; 17:945–950.
28. Bao C, Chen W, Weir MD, Thein-Han W, Xu HHK. Effects of electrospun submicron fibers in calcium phosphate cement scaffold on mechanical properties and osteogenic differentiation of umbilical cord stem cells. Acta Biomaterialia. 2011; 7:4037–4044. [PubMed: 21763791]
29. Zuo Y, Yang F, Wolke JG, Li Y, Jansen JA. Incorporation of biodegradable electrospun fibers into calcium phosphate cement for bone regeneration. Acta Biomaterialia. 2010; 6:1238–1247. [PubMed: 19861181]
30. Blom EJ, Klein-Nulend J, Wolke JG, Kurashina K, van Waas MA, Burger EH. Transforming growth factor-beta1 incorporation in an alpha-tricalcium phosphate/dicalcium phosphate dihydrate/tetracalcium phosphate monoxide cement: release characteristics and physicochemical properties. Biomaterials. 2002; 23:1261–1268. [PubMed: 11794323]
31. Simmons CA, Alsberg E, Hsiong S, Kim WJ, Mooney DJ. Dual growth factor delivery and controlled scaffold degradation enhance in vivo bone formation by transplanted bone marrow stromal cells. Bone. 2004; 35:562–569. [PubMed: 15268909]
32. Jansen JA, Vehof JWM, Ruhe PQ, Kroeze-Deutman H, Kuboki Y, Takita H, Hedberg EL, Mikos AG. Growth factor-loaded scaffolds for bone engineering. J Controlled Release. 2005; 101:127–136.
33. Kaigler D, Krebsbach PH, Wang Z, West ER, Horger K, Mooney DJ. Transplanted endothelial cells enhance orthotopic bone regeneration. J Dent Res. 2006; 85:633–637. [PubMed: 16798864]
34. Shi X, Sitharaman B, Pham QP, Liang F, Wu K, Billups WE, Wilson LJ, Mikos AG. Fabrication of porous ultra-short single-walled carbon nanotube nanocomposite scaffolds for bone tissue engineering. Biomaterials. 2007; 28:4078–4090. [PubMed: 17576009]
35. Kuo CK, Ma PX. Ionically crosslinked alginate hydrogels as scaffolds for tissue engineering: Part I. Structure, gelation rate and mechanical properties. Biomaterials. 2001; 22:511–521. [PubMed: 11219714]
36. Drury JL, Dennis RG, Mooney DJ. The tensile properties of alginate hydrogels. Biomaterials. 2004; 25:3187–3199. [PubMed: 14980414]
37. Drury JL, Mooney DJ. Hydrogels for tissue engineering: scaffold design variables and applications. Biomaterials. 2003; 24:4337–4351. Review. [PubMed: 12922147]
38. Damien CJ, Parsons JR. Bone graft and bone graft substitutes: A review of current technology and applications. J Appl Biomater. 1991; 2:187–208. [PubMed: 10149083]
39. O'Kelly K, Tancred D, McCormack B, Carr A. A quantitative technique for comparing synthetic porous hydroxyapatite structure and cancellous bone. J Mater Sci: Mater in Med. 1996; 7:207–213.
40. Nalla RK, Stolken JS, Kinney JH, Ritchie RO. Fracture in human cortical bone: localfracture criteria and toughening mechanisms. J Biomechanics. 2005; 38:1517–1525.
41. Flautre B, Delecourt C, Blary MC, Van Landuyt P, Lemaitre J, Hardouin P. Volume effect on biological properties of a calcium phosphate hydraulic cement: experimental study in sheep. Bone. 1999; 25(Suppl):35S–39S. [PubMed: 10458272]
42. Bodde EW, Boerman OC, Russel FG, Mikos AG, Spauwen PH, Jansen JA. The kinetic and biological activity of different loaded rhBMP-2 calcium phosphate cement implants in rats. J Biomed Mater Res A. 2008; 87:780–791. [PubMed: 18200544]
43. Pan Z, Jiang P. Assessment of the suitability of a new composite as a bone defect filler in a rabbit model. J Tissue Eng Regen Med. 2008; 2:347–353. [PubMed: 18612971]
44. Ikenaga M, Hardouin P, Lemaitre J, Andrianjatovo H, Flautre B. Biomechanical characterization of a biodegradable calcium phosphate hydraulic cement: a comparison with porous biphasic calcium phosphate ceramics. J Biomed Mater Res. 1998; 40:139–144. [PubMed: 9511108]
45. Gerstenfeld LC, Cullinane DM, Barnes GL, Graves DT, Einhorn TA. Fracture healing as a post-natal developmental process: molecular, spatial, and temporal aspects of its regulation. J Cell Biochem. 2003; 88:873–884. [PubMed: 12616527]

46. Chung YI, Ahn KM, Jeon SH, Lee SY, Lee JH, Tae G. Enhanced bone regeneration with BMP-2 loaded functional nanoparticle-hydrogel complex. J Control Release. 2007; 121:91–99. [PubMed: 17604871]
47. Seeherman HJ, Azari K, Bidic S, Rogers L, Li XJ, Hollinger JO, et al. rhBMP-2 delivered in a calcium phosphate cement accelerates bridging of critical-sized defects in rabbit radii. J Bone Joint Surg Am. 2006; 88:1553–1565. [PubMed: 16818982]
48. Rodeo SA. What's new in orthopaedic research. J Bone Joint Surg Am. 2003; 85-A(10):2054–2062. [PubMed: 14563819]
49. Chen G, Deng C, Li YP. TGF-beta and BMP signaling in osteoblast differentiation and bone formation. Int J Biol Sci. 2012; 8:272–288. [PubMed: 22298955]
50. Wara AK, Foo S, Croce K, Sun X, Icli B, Tesmenitsky Y, et al. TGF-beta1 signaling and Kruppel-like factor 10 regulate bone marrow-derived proangiogenic cell differentiation, function, and neovascularization. Blood. 2011; 118:6450–6460. [PubMed: 21828131]
51. Kempen DH, Lu L, Heijink A, Hefferan TE, Creemers LB, Maran A, et al. Effect of local sequential VEGF and BMP-2 delivery on ectopic and orthotopic bone regeneration. Biomaterials. 2009; 30:2816–2825. [PubMed: 19232714]
52. Jiang J, Fan CY, Zeng BF. Experimental Construction of BMP2 and VEGF Gene Modified Tissue Engineering Bone in Vitro. Int J Mol Sci. 2011; 12:1744–1755. [PubMed: 21673920]
53. Ferrara N, Gerber HP, LeCouter J. The biology of VEGF and its receptors. Nat Med. 2003; 9:669–676. [PubMed: 12778165]
54. Deckers MM, Karperien M, van der Bent C, Yamashita T, Papapoulos SE, Lowik CW. Expression of vascular endothelial growth factors and their receptors during osteoblast differentiation. Endocrinology. 2000; 141:1667–1674. [PubMed: 10803575]
55. Uludag H, D'Augusta D, Golden J, Li J, Timony G, Riedel R, Wozney JM. Implantation of recombinant human bone morphogenetic proteins with biomaterials: correlation between protein pharmacokinetics and osteoinduction in rat ectopic model. J Biomed Mater Res. 2000; 50:227–238. [PubMed: 10679688]
56. Ruhé PO, Boerman OC, Russel FGM, Mikos AG, Spauwen PHM, Jansen JA. In vivo release of rhBMP-2 loaded porous calcium phosphate cement pretreated with albumin. J Mater Sci: Mater Med. 2006; 17:919–927. [PubMed: 16977389]
57. Ziegler J, Anger D, Krummenauer F, Breitig D, Fickert S, Guenther KP. Biological activity of recombinant human growth factors released from biocompatible bone implants. J Biomed Mater Res A. 2008; 86:89–97. [PubMed: 17941024]
58. Wang X, Ma J, Feng QL, Cui FZ. In vivo evaluation of s-chitosan enhanced calcium phosphate cements. J Bioactive Compatible Polymers. 2003; 18:259–271.

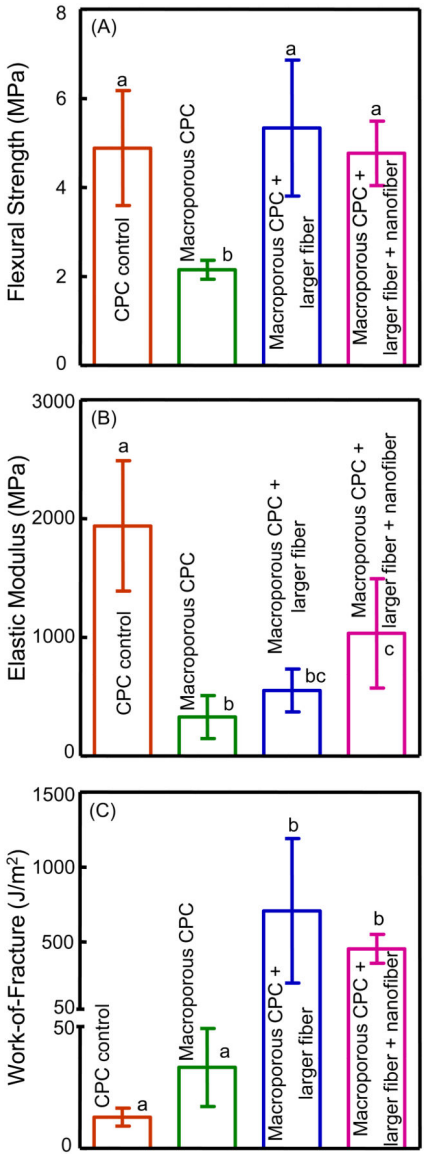

Figure 1.

Mechanical properties of CPC scaffolds: (A) Flexural strength, (B) elastic modulus, and (C) work-of-fracture (toughness) (mean ± sd; n = 6). Creating macropores in CPC lowered the strength, when comparing the first group with the second group. Fiber reinforcement increased the strength of macroporous CPCs (comparing the third and fourth groups with the second group), which matched the strength of control CPC without macropores. In each plot, values with dissimilar letters are significantly different from each other ($p < 0.05$).

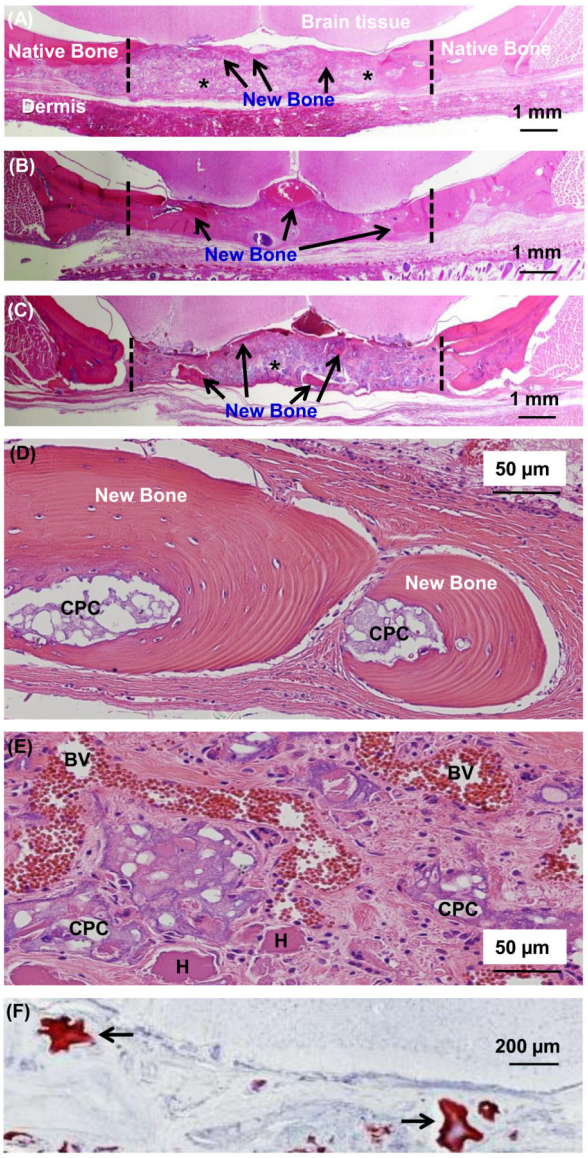

Figure 2.

Representative H&E staining images of samples harvested from the cranial defects of rats: (A) Example for group 3 at 24 weeks, (B) group 5 at 24 weeks, (C) group 6 at 24 weeks, (D) example of new bone centering around CPC residues for group 1, (E) blood vessels in the fibrous connective tissue in the defect area of group 2, and (F) alginate residues in the defect area for group 4. New bone had grown inward toward the defect center. In (A-C), the dotted lines indicate the approximate boundaries of the original defect, remnants of CPC were labeled with *, and black arrows highlight the presence of new bone formation. In (E), BV indicates blood vessels. H indicates alginate hydrogel residues. Other groups had similar blood vessels formation. In (F), alginate residuals were indicated by arrows and stained red with Safranin O staining.

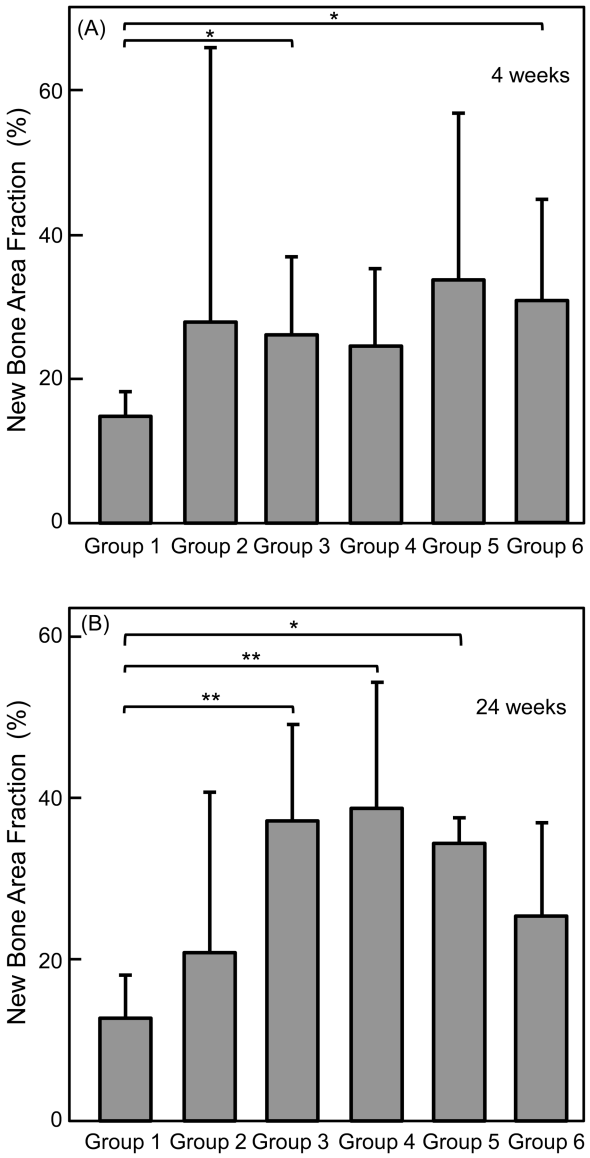

Figure 3.

Area fraction of new bone in cranial defects measured from the H&E staining images (mean ± sd; n = 5): (A) 4 weeks, and (B) 24 weeks. The new bone and original implantation areas in the H&E staining images were calculated by Image J (NIH) software. For each defect, the new bone area fraction = new bone area/original total implant area. In each plot, values indicated with * are significantly different from each other ($p < 0.05$).

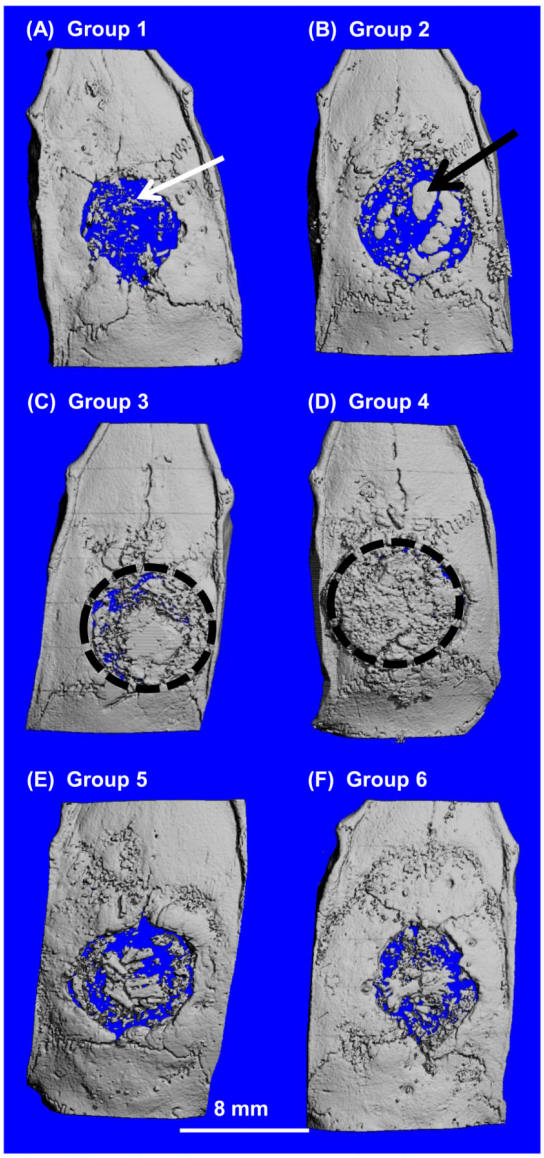

Figure 4.

Examples of μCT images of cranial defects for the 6 groups at 24 weeks. White arrow in (A) indicates CPC material. Black arrow in (B) indicates new bony islands. In (C) and (D), the defect was almost completely bridged with new bone, where the dotted black circle indicates the original defect area that had been filled with newly formed bone. It should be noted that each group had variations in the samples, ranging from less new bone (such as those in A and B), to intermediate amounts of new bone (such as those in E and F), to relatively high amounts of new bone (such as those in C and D).